Received November 7, 2020, accepted November 22, 2020, date of publication November 26, 2020,
date of current version December 11, 2020.

Digital Object Identifier 10.1109/ACCESS.2020.3040960

Pulse Position Detection of the Pseudo Random Time-Hopping Pseudolite for the Participative GNSS Receivers

YI HU[1,2], BAOGUO YU[2], MAOZHONG SONG[3], AND ZHIXIN DENG[2]
[1]School of Mechanical and Electrical Engineering, Chuzhou University, Chuzhou 239000, China
[2]State Key Laboratory of Satellite Navigation System and Equipment Technology, Shijiazhuang 050081, China
[3]College of Electronic and Information Engineering, Nanjing University of Aeronautics and Astronautics, Nanjing 210016, China

Corresponding author: Yi Hu (hygps607@163.com)

This work was supported in part by the Open Research Fund of State Key Laboratory of Satellite Navigation System and Equipment Technology under Grant CEPNT-2017KF-06, and in part by the Natural Science Foundation of the Anhui Higher Education Institutions under Grant KJ2018A0427.

ABSTRACT The pulse position detection of the pseudorandom time-hopping (TH) pseudolite is critical for the participative global navigation satellite system (GNSS) receivers. The conventional method to detect the pseudorandom TH pulse positions of the received pseudolite signal is mainly based on the exhaustive search of the matched TH intervals, which may cause low detection probability or even detection failure in relatively low signal to noise ratio (SNR) environments. With this problem, a new method to detect the TH pulse positions is given. The general process of the given method is that first the TH intervals derived from the correlation peaks of discontinuous direct sequence spread spectrum (DSSS) component are mapped to a code sequence, and then the mapped code sequence is circularly correlated in turn with each code sequence obtained from each group of TH slot indices of the TH table, finally by searching the maximum circular correlation peak, the TH slot indices of the received pseudolite signal and their initial phase will be found, further by combining them the work of TH pulse position detection is fulfilled. The simulation results show that with the given method, the detection probability and detection error of the obtained TH pulse positions can be greatly improved, hence the performance of the participative GNSS receivers will be enhanced.

INDEX TERMS Pseudorandom time-hopping pseudolite, participative GNSS receiver, pulse position detection, mapped code sequence, circular correlation.

I. INTRODUCTION

The pseudolite can be used to augment the navigation and positioning performance of the participative GNSS receivers in environments as interior of the building, city crayon, mountain valleys and so on, where the number of the visible GNSS satellites decreases dramatically [1]–[3]. Meanwhile, four or more pseudolites can also be used to constitute an independent positioning system in environments where the received GNSS satellite signals are virtually blocked or jammed [4], [5]. Since the distance from the pseudolite to GNSS receivers is much closer than that of the navigation satellites in the sky, the received power of the pseudolite signal is much stronger than that of the navigation satellites, and this will bring the ''near-far'' interference to GNSS receivers [6], [7]. To solve this problem, most pseudolites often adopt the signal structure of pseudorandom TH pulses gating continuous DSSS signal [8]–[10]. The duty cycle of TH pulses is predetermined and pulse positions are controlled by a group of pseudorandom TH slot indices which can be generated by a linear feedback shift register (LFSR) [11], [12] or by a stored TH table [13]–[15]. The role of the pseudorandom TH slot indices is to maintain the spectral characteristics of original continuous DSSS signal so that the Doppler frequency ambiguity appeared in acquisition and tracking of the pseudolite signal can be removed [8], [15], [16]. Generally speaking, a TH table is relatively convenient for use than the LFSR-based method, since that the pulse number in one TH pulse pattern controlled by a LFSR may not easily meet the pulse number given in advance.

For the received pseudolite signal, due to time delay its TH pulse positions are determined by the pseudorandom noise (PRN) code initial phase of discontinuous DSSS component and the initial phase of TH slot indices. The conventional method to detect the TH pulse positions of the received pseudolite signal is mainly based on the exhaustive search of the matched TH intervals [17]–[19]. In [17], it uses the sliding correlation method to detect and demodulate the

The associate editor coordinating the review of this manuscript and approving it for publication was Masood Ur-Rehman.

pulsed pseudolite signal, and this sliding correlation is just an exhaustive strategy. In [18] a heuristic method to detect the TH pulse positions is proposed, in the given method it acquires the TH pulse positions by exhaustively searching the TH intervals or hops and comparing them with the intervals of TH slot indices derived from the TH table. In [19], two methods, namely, maximum likelihood estimation (MLE) method and non-coherent squaring detection (NSD) method, are used to detect the TH pulse positions. For the MLE method, it uses a group of match filters to detect the pulse positions and its detection process is similar to that given in [18]. While for the NSD method, it regards the pulse positions as a sequence of independent random variables and uses the generalized likelihood ratio test (GLRT) approach to detect the TH pulse positions, and this can simplify the detection process of the MLE method. By comparisons, it shows that the MLE method is superior to the NSD method in detection performance, but its computational efficiency is inferior to the latter.

In general, the drawback of this exhaustive search method is that it may cause low detection probability or even detection failure when some obtained TH intervals get wrong, especially in low SNR environments. In fact, these obtained TH intervals can be also mapped into code sequence so that the circular correlation method can be used to decrease the effect of some unmatched TH intervals. In [15], during the course of a method is given to improve the acquiring efficiency of the pulsed TH pseudolite signal, a similar idea that uses the timeslots mapped code sequence to search the TH slot indices is mentioned. While for the LFSR-based methods, though they can be easily used to detect the TH pulse positions with the TH code sequence generated by the local LFSR of the participative GNSS receiver [11], [12], their detection process is different in different pulse scheme, so in the following parts they are not considered.

Aim at the problem of the exhaustive search method, in this paper a new method to detect the pseudorandom TH pulse positions of the received pseudolite signal with better performance is given. The general process of the given method consists of three steps. Firstly, the autocorrelation peak positions of discontinuous DSSS component are acquired and the code sequence mapped from the autocorrelation peak intervals is derived. Secondly, by operating on the TH table, different code sequences mapped from different groups of TH slot indices are got. Finally, the code sequence derived in first step is circularly correlated in turn with each mapped code sequence of the TH table got in second step, and by finding the maximum circular correlation peak, the TH slot indices and their initial phase will be found, further by combining them the task of TH pulse position detection is fulfilled. The simulations presented in the final of the paper show that compared with the exhaustive search method, the TH pulse position detection performance can be greatly improved with the given method.

The rest of the paper is organized as follows. In Section II, the received signal model of the pseudorandom TH pseudolite is first given. Then in Section III, the detailed TH pulse position detection process is presented. In Section IV, different simulations to validate the given method are shown. Finally, the paper is concluded in Section V.

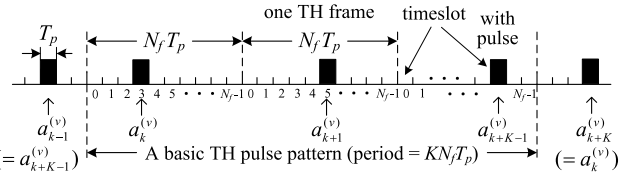

FIGURE 1. Signal structure of the pseudorandom TH pseudolite in transmitting end.

Group ID	TH slot index in different frame ($0 - K$-1) of one basic pulse pattern				
	0	**1**	**2**	· · ·	***K*-1**
1	$a_0^{(1)}$	$a_1^{(1)}$	$a_2^{(1)}$	· · ·	$a_{K-1}^{(1)}$
2	$a_0^{(2)}$	$a_1^{(2)}$	$a_2^{(2)}$	· · ·	$a_{K-1}^{(2)}$
⋮	⋮	⋮	⋮	⋮	⋮
***v*-1**	$a_0^{(v-1)}$	$a_1^{(v-1)}$	$a_2^{(v-1)}$	· · ·	$a_{K-1}^{(v-1)}$
***v* (used)**	$a_0^{(v)}$	$a_1^{(v)}$	$a_2^{(v)}$	· · ·	$a_{K-1}^{(v)}$
***v*+1**	$a_0^{(v+1)}$	$a_1^{(v+1)}$	$a_2^{(v+1)}$	· · ·	$a_{K-1}^{(v+1)}$
⋮	⋮	⋮	⋮	⋮	⋮
N	$a_0^{(N)}$	$a_1^{(N)}$	$a_2^{(N)}$	· · ·	$a_{K-1}^{(N)}$

FIGURE 2. The TH table used to generate and detect the TH slot indices of the pseudolite signal.

II. RECEIVED SIGNAL MODEL OF THE PSEUDO RANDOM TH PSEUDOLITE

A. SIGNAL STRUCTURE OF THE PSEUDORANDOM TH PSEUDOLITE

The signal structure of the pseudorandom TH pseudolite is depicted as Fig. 1, where $N_f = 1/d$ is the slot number in one TH frame, and here d is the duty cycle of the pseudolite signal; T_p is the period of one TH pulse; k is the current TH frame index and K is the frame number in one TH pulse pattern; $\left\{a_{k+i}^{(v)}\right\}_{i=0}^{K-1}$ is a basic TH slot index set of the v-th group in TH table used by the pseudolite signal, where $a_{k+i}^{(v)}$ meets: (i) $a_{k+i}^{(v)} \in \{0, 1, \ldots, N_f - 1\}$ is a random number, and if $K = N_f$, $\left\{a_{k+i}^{(v)}\right\}_{i=0}^{K-1}$ will become a full random permutation of 0 to $K - 1$ (the trivial permutation as 0 to $K - 1$ or reverse should be avoided [10]); (ii) for any given i, $a_{k+i}^{(v)} = a_{k+i+K}^{(v)}$, $i = 0, 1, 2, \ldots, K - 1$; (iii) $a_{k+i}^{(v)} \neq a_{k+j}^{(v)}$ when $i \neq j$, $i, j = 0, 1, \ldots, K - 1$; (iv) if there is another pseudolite signal which uses the w-th group TH slot indices in TH table, then for the non-overlap pulse scheme, there will have $a_{k+i}^{(v)} \neq a_{k+i}^{(w)}$, where $v \neq w$ and $i = 0, 1, 2, \ldots, K - 1$. Here the TH table used by the pseudolite is shown as Fig. 2.

B. RECEIVED SIGNAL MODEL OF THE PSEUDO RANDOM TH PSEUDOLITE

Base on Figs. 1 and 2, the received pseudolite signal after down-conversion can be written as

$$r(t) = \sqrt{2P}\sum_{n=-\infty}^{+\infty} \times \sum_{m=0}^{M-1}\left(\begin{array}{l} b_n \cos\left[2\pi(f_{IF}+f_{Dop})t+\varphi_0\right] \\ \times s\left(t-nT_b\right)p^{(v)}(t-nT_b-mT_c-\tau_c)\end{array}\right)+n(t) \tag{1}$$

where P is the power of the received pseudolite signal; b_n is the transmitted data bit and $b_n \in \{-1,+1\}$ with equal probability; T_b and T_c are respectively the periods of data bit and PRN code chip; f_{IF}, f_{Dop}, and φ_0 are intermediate frequency (IF), Doppler frequency, and initial phase of the carrier, respectively; $n(t)$ is the additive white noise; $s(t)$ is the baseband signal, $p^{(v)}(t)$ is the TH gating pulse whose position is assigned with the v-th group TH slot indices in TH table, and they can be formulated by

$$s(t) = \sum_{m=0}^{M-1} c_m u_{T_c}\left(t-mT_c-\tau_c\right), \tag{2}$$

$$p^{(v)}(t) = \sum_{k=-\infty}^{+\infty} u_{T_p}\left(t-a_k^{(v)}T_p-kN_fT_p\right) \tag{3}$$

where $c_m \in \{-1,+1\}$ is the PRN code of DSSS signal, and M is the code number in one code period; $a_k^{(v)}$ is the pseudorandom TH slot index which has been elaborated in Subsection II-A; T_p is the period of TH pulses or timeslots, and often it meets $T_p = MT_c$; τ_c is the PRN code initial phase; $u_T(t)$ is a unit-height rectangle pulse whose support is on the range $[0, T]$. Here the relationships of T_b, T_p and T_c are shown in Fig. 3, where the TH slot indices in P_α are not same as those in P_β ($\alpha, \beta = 0, 1, \ldots, N_b$-1).

III. PULSE POSITION DETECTION OF THE PSEUDO RANDOM TH PSEUDOLITE

A. THE ROLE OF TH PULSE POSITION DETECTION

The role of TH pulse position detection mainly lies in two aspects: (i) to provide time delay of the TH pulse positions for the ranging of the participative GNSS receivers; (ii) to provide pulse demodulation information for the participa-tive GNSS receivers so that the effect of the TH pulses can be removed.

In essence, TH pulse position detection is to find the initial phase or time delay τ_p of the pseudorandom TH pulses, and it can be realized by measuring the current TH pulse position relative to its original position, as shown in Fig. 4.

On the other hand, from Fig. 4 it shows that the time delay τ_p consists of two parts, i.e., the integral part τ_{ip} and the fractional part τ_{fp} which are both in unit of timeslot. In fact, by analysis it is found that τ_{fp} is just the PRN code initial phase of the DSSS component, and it can be

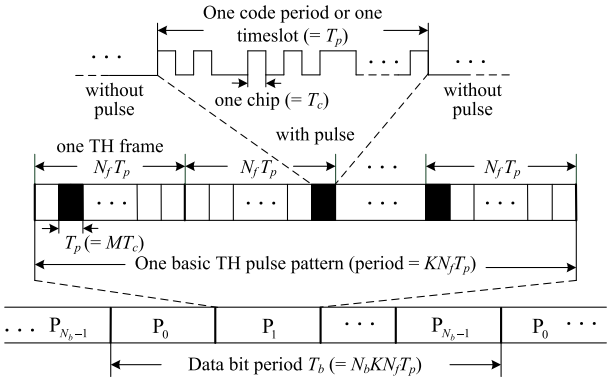

FIGURE 3. The relationships of T_b, T_p and T_c in Eqs. (1) to (3).

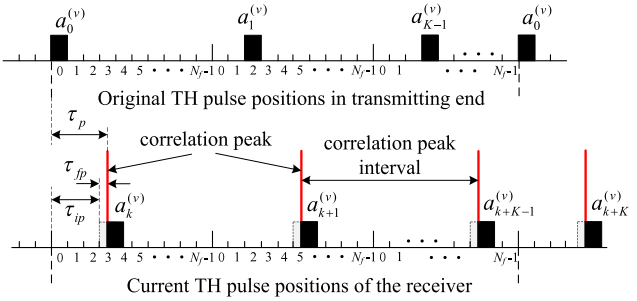

FIGURE 4. The detection of TH pulse positions can be fulfilled by measuring the initial phase τ_{ip} and τ_{fp} which are both related with the autocorrelation peak positions of discontinuous DSSS component.

obtained by the autocorrelation peak positions derived from the acquired result of the DSSS component. Moreover, aided with the obtained autocorrelation peak positions, τ_{ip} can also be obtained with the method given in the following Subsections III-C to III-E.

B. ACQUIRING OF THE PRN CODE INITIAL PHASE OF DSSS COMPONENT

Though the DSSS component of the received TH pseudolite signal is discontinuous, the method for acquiring the PRN code initial phase of continuous GNSS satellite signal still can be used to acquire the PRN code initial phase of TH pseudolite signal [18], [20]. Often the known parallel PRN code phase acquisition method [21], [22] can be chosen to fulfill this work.

With the chosen acquisition method, the PRN code initial phase or time delay τ_{fp} of the TH pseudolite signal can be acquired by

$$\tau_{fp} = \arg\left(\max_{\hat{\tau}_c,\hat{f}_{Dop}} \sqrt{I_{\hat{c}_m}^2(\hat{\tau}_c,\hat{f}_{Dop})+Q_{\hat{c}_m}^2(\hat{\tau}_c,\hat{f}_{Dop})}\right) \tag{4}$$

where $I_{\hat{c}_m}(\hat{\tau}_c,\hat{f}_{Dop})$ and $Q_{\hat{c}_m}(\hat{\tau}_c,\hat{f}_{Dop})$ are in-phase and quadrature integration results of the participative GNSS receiver, respectively, and

$$I_{\hat{c}_m}(\hat{\tau}_c,\hat{f}_{Dop}) = \sqrt{2}\int_0^{2N_fT_p} r(t)s_{\hat{c}_m}(\hat{\tau}_c)\cos\left[2\pi(f_{IF}+\hat{f}_{Dop})t+\hat{\varphi}_0\right]dt, \tag{5}$$

$$Q_{\hat{c}_m}(\hat{\tau}_c, \hat{f}_{Dop}) = \sqrt{2}\int_0^{2N_f T_p} r(t) s_{\hat{c}_m}(\hat{\tau}_c) \sin\left[2\pi(f_{IF} + \hat{f}_{Dop})t + \hat{\varphi}_0\right] dt \tag{6}$$

where $\{\hat{c}_m\}_{m=0}^{M-1}$, $\hat{\tau}_c$, $\hat{f}_{Dop}$, and $\hat{\varphi}_0$ are PRN code sequence, initial phase of PRN code sequence, Doppler frequency, and carrier initial phase of local generated TH pseudolite signal, respectively; $s_{\hat{c}_m}(\hat{\tau}_c) = \sum_{m=0}^{M-1} \hat{c}_m u_{T_c}\left(t - mT_c - \hat{\tau}_c\right)$ is the baseband signal with the obtained code sequence $\{\hat{c}_m\}_{m=0}^{M-1}$ and its initial phase $\hat{\tau}_c$. Here the integration period chosen as $2N_f T_p$ is to ensure that at least one pulse is existed when time delay of the pseudorandom TH pulses is considered.

In practice, FFT algorithm can be used to acquire the PRN code initial phase, and $\hat{f}_{Dop}$ used in Eq. (4) can be set to 0 to decrease the computational load [19]. Additionally, to avoid the autocorrelation peak loss arisen from the improper data segmentation of the FFT algorithm [12], the overlap-adding based digital passive matched filtering (DPMF) [18] method can be used instead.

C. CODE SEQUENCE MAPPED FROM AUTOCORRELATION PEAK INTERVALS

Although the TH slot indices of the pseudolite signal is changed randomly, the timeslot width of the psedolite signal is unchanged. Thus each timeslot can be taken as a "sampling" point with value 1 or 0 in view of the slot with or without TH pulse, respectively. By this the received pseudolite signal can be mapped into a code sequence, which will bring benefit to the TH pulse position detection.

With the PRN code initial phase τ_{fp} obtained above, the estimated baseband signal can be written as $s_{\hat{c}_m}(\tau_{fp}) = \sum_{m=0}^{M-1} \hat{c}_m u_{T_c}\left(t - mT_c - \tau_{fp}\right)$. Substitute $s_{\hat{c}_m}(\tau_{fp})$ into Eqs. (5) and (6), meanwhile, change the integral intervals of Eqs. (5) and (6) from $[0,\ 2N_f T_p]$ to $[\kappa N_f T_p,\ (\kappa+1)N_f T_p]$, where $\kappa = 0, 1, \ldots, \lfloor \Delta t / (N_f T_p) \rfloor - 1$, and here Δt is the time span of signal collection and $\lfloor \cdot \rfloor$ denotes the floor operation, thus by comparing the maximum values of $\sqrt{I^2_{\hat{c}_m}(\kappa, \tau_{fp}, \hat{f}_{Dop}) + Q^2_{\hat{c}_m}(\kappa, \tau_{fp}, \hat{f}_{Dop})}$ where $\kappa = 0, 1, \ldots, \lfloor \Delta t / (N_f T_p) \rfloor - 1$, the autocorrelation peaks of DSSS component and their positions can be easily found. Similarly, this correlation process can be also implemented with the segmented overlap-adding FFT algorithm to improve efficiency.

Suppose N_t autocorrelation peaks have been found and their positions are $\{p_k, k = 0, 1, 2, \ldots, N_t - 1\}$, thus the autocorrelation peak intervals in unit of timeslot or T_p can be given as

$$\Lambda_{k-1,k} = \left\lfloor \frac{p_k - p_{k-1}}{T_p f_s} \right\rfloor, \quad k = 1, 2, \ldots, N_t - 1 \tag{7}$$

where f_s is the sampling frequency.

If the autocorrelation peak intervals given in Eq. (7) are directly used to search the original TH slot indices of the pseudolite signal in TH table, some unmatched autocorrela-tion peak intervals can cause low detection probability or even detection failure, especially when SNR of the received pseudolite signal is relatively low. To improve this problem, the code sequence mapped from the autocorrelation peak intervals can be used to search the original TH slot indices.

With Eq. (7) the autocorrelation peak interval set can be easily written as $\{\Lambda_{k-1,k}, k = 1, 2, \ldots, N_t - 1\}$, thus the mapped code sequence can be given by $\mathbf{H} = \left\{h(i), i = 0,\ 1, \ldots, \sum_{k=1}^{N_t-1} \Lambda_{k-1,k}\right\}$ where

$$h(i) = \begin{cases} 1, & i = 0 \\ 1, & i = \sum_{k=1}^{J} \Lambda_{k-1,k},\ J = 1, 2, \ldots, N_t - 1 \\ 0, & others. \end{cases} \tag{8}$$

To improve the gain of the following circular correlation operation, in application the code sequence $\mathbf{H}$ can be further interpolated to form its expanded result $\bar{\mathbf{H}}$. More specifically, suppose the interpolation factor is I, then $\bar{\mathbf{H}}$ is given as that at the bottom of this page.

D. CODE SEQUENCE MAPPED FROM TH SLOT INDICES

Similar as the derivation of the code sequence mapped from the autocorrelation peak intervals, each group of TH slot indices given in TH table can also be mapped into a code sequence for the subsequent TH pulse position detection.

To get the code sequences mapped from the TH slot indices of the whole TH table, first the ζ-th group TH slot indices in the TH table are chosen to illustrate how to map them into a code sequence. According to the structure of TH slot indices described in Subsection II-A, the mapped code sequence of the ζ-th group can be given as $\Gamma^{(\zeta)} = \{\gamma^{(\zeta)}(i), i = 0, 1, \ldots, KN_f - 1\}$, where $\zeta = 1, 2, \ldots, N$ and

$$\gamma^{(\zeta)}(i) = \begin{cases} 1, & i = a_j^{(\zeta)}, j = 0, 1,\ \ldots, K-1 \\ 0, & others. \end{cases} \tag{9}$$

Operating similarly as in Subsection III-C, the code sequence $\Gamma^{(\zeta)}$ can also be interpolated to form its expanded

$$\bar{\mathbf{H}} = \Bigg[\underbrace{h(0), \ldots, h(0)}_{I}, \underbrace{h(1), \ldots, h(1)}_{I}, \ldots, \underbrace{h(\sum_{k=1}^{N_t-1} \Lambda_{k-1,k}), \ldots, h(\sum_{k=1}^{N_t-1} \Lambda_{k-1,k})}_{I}\Bigg].$$

result $\bar{\mathbf{\Gamma}}^{(\zeta)}$ with the same interpolation factor for $\bar{\mathbf{H}}$. Then the mapped code sequences of the whole TH table can be given as

$$\bar{\mathbf{\Gamma}} = \left[\left(\bar{\mathbf{\Gamma}}^{(1)}\right)', \left(\bar{\mathbf{\Gamma}}^{(2)}\right)', \ldots, \left(\bar{\mathbf{\Gamma}}^{(\zeta)}\right)', \ldots, \left(\bar{\mathbf{\Gamma}}^{(N)}\right)'\right]' \quad (10)$$

where the superscript " ' " denotes the transpose.

E. TH PULSE POSITION DETECTION

After obtaining the mapped code sequences of $\bar{\mathbf{H}}$ and $\bar{\mathbf{\Gamma}}$, the circular correlation method and the FFT algorithm can be used to find the TH slot indices and their initial phase of the received pseudolite signal.

To apply the circular correlation method and the FFT algorithm, first $\bar{\mathbf{H}}$ and each vector $\bar{\mathbf{\Gamma}}^{(\zeta)}$ $(\zeta = 1, 2, \ldots, N)$ should be aligned to the same length. Often the length of $\bar{\mathbf{H}}$ is greater than that of $\bar{\mathbf{\Gamma}}^{(\zeta)}$ so that the TH slot indices and their initial phase of the pseudolite signal can be correctly detected. Suppose the length of $\bar{\mathbf{H}}$ is L, then the aligned vector of ζ-th group $\bar{\mathbf{\Gamma}}^{(\zeta)}$ will become $\tilde{\Gamma}^{(\zeta)} = \left[\underbrace{\bar{\mathbf{\Gamma}}^{(\zeta)}, \bar{\mathbf{\Gamma}}^{(\zeta)}, \ldots, \bar{\mathbf{\Gamma}}^{(\zeta)}}_{\ell \text{ groups}}, \bar{\Gamma}'^{(\zeta)}\right]$ where $\ell = \left\lfloor L/(KN_f) \right\rfloor$ and $\bar{\Gamma}'^{(\zeta)}$ is a vector whose elements are selected from the first $L - \ell K N_f$ elements of $\bar{\mathbf{\Gamma}}^{(\zeta)}$ in sequence. Continue to align the other vectors of $\bar{\mathbf{\Gamma}}$ similarly as $\tilde{\Gamma}^{(\zeta)}$, finally the whole aligned code sequences can be got as $\tilde{\Gamma} = \left[(\tilde{\Gamma}^{(1)})', (\tilde{\Gamma}^{(2)})', \ldots, (\tilde{\Gamma}^{(\zeta)})', \ldots, (\tilde{\Gamma}^{(N)})'\right]'$.

With the obtained code sequences $\bar{\mathbf{H}}$ and $\tilde{\Gamma}$, the detected TH slot indices and their initial phase in sampling points can be finally obtained by

$$p^{(\hat{\zeta})} = \arg\left(\max_{\substack{i=0,1,\ldots,L-1;\\ \zeta=1,2,\ldots,N}} \max \left(\bar{\mathbf{H}}(i) \otimes \tilde{\Gamma}^{(\zeta)}(i)\right)\right) \quad (11)$$

where $\hat{\zeta}$ is the estimation of ζ, and it denotes the detected group ID of TH slot indices in TH table; $\bar{\mathbf{H}}(i)$ and $\tilde{\Gamma}^{(\zeta)}(i)$ denotes the code sequences of $\bar{\mathbf{H}}$ and $\tilde{\Gamma}^{(\zeta)}$ after circularly shifting i mapped codes; "$\otimes$" and "maxmax" denote the circular correlation and max-max operations, respectively.

To improve efficiency, the detection of $p^{(\hat{\zeta})}$ given in Eq. (11) can also be implemented with FFT algorithm and its detailed process is

$$p^{(\hat{\zeta})} = \arg\left(\max_{\substack{i'=0,1,\ldots,L-1;\\ \zeta=1,2,\ldots,N}} \max \left|\mathrm{IFFT}^{(i')}\left\{\mathrm{FFT}(\bar{\mathbf{H}}) \cdot \mathrm{conj}\left[\mathrm{FFT}(\tilde{\Gamma}^{(\zeta)})\right]\right\}\right|\right) \quad (12)$$

where "conj" and "$|\cdot|$" denote conjugate and absolute operations, respectively, and i' is the column index of the IFFT sequence.

Using $p^{(\hat{\zeta})}$ given by Eq. (11) or (12), the initial phase τ_{ip} can be easily got as $\tau_{ip} = p^{(\hat{\zeta})} / (f_s T_p)$. Then with τ_{ip} and the previous τ_{fp} given by Eq. (4), TH pulse positions of the pseudolite can be easily obtained by $\tau_p = \tau_{ip} + \tau_{fp}$ and the detected $\hat{\zeta}$-th group TH slot indices.

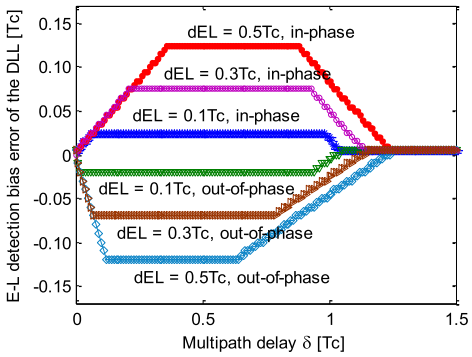

FIGURE 5. The detection bias error of the early (E) and late (L) correlators of the DLL under different multipath delay and different E-L spacing (dEL), in which the amplitude ratio of the multipath to the LOS signal is 0.5.

F. SOME DISCUSSIONS ON THE GIVEN METHOD

1) THE EFFECT OF THE MULTIPATH

Besides the aforementioned "near-far" interference, the multipath arises from the pseudolite signal reflection or diffraction by the tall buildings, trees and so on may also cause the performance degradation of the participative GNSS receivers [1]. In what follows, we will mainly discuss the effect of the multipath on the TH pulse detection, and the detailed method of multipath mitigation is out of the scope of this paper.

Based on the TH pulse position detection process given in Subsection III-A, it is known that the effect of the multipath on the TH pulse detection can be boiled down to the effect on the initial phase τ_p, which further includes the effect on the fractional part τ_{fp} and on the integral part τ_{ip}.

a) For τ_{fp}, the effect of the multipath on the pseudolite is just same as it on the normal GNSS satellite signal. That is, only when the time delay of the multipath is less than about one PRN code chip or T_c, the detection of τ_{fp} will be affected dramatically. Through the analysis given in [22], it shows that the maximum detection error caused by the multipath is about one quarter spacing of the early (E) and late (L) correlators of the delay locked loop (DLL). On the other hand, at this time the effect of the multipath can be mitigated by the hardware such as narrow correlator or high resolution correlator (HRC) [23], multipath estimating DLL (MEDLL) [24] and so on, or by the post processing techniques such as the fast iterative maximum likelihood algorithm (FIMLA) [25] and so on. At the time when there exists one multipath, the detection bias error under different multipath delay and different spacing (dEL) of the E and L correlators are shown as Fig. 5. In practice, the narrow spacing correlators (e.g., dEL $\leq 0.1T_c$) are often used so that the better multipath mitigation performance can be got.

b) For τ_{ip}, the multipath can cause the incorrect peak interval judgment which will further lead to the wrong detected result of τ_{ip}. But this effect can be easily removed after a simple peak merging processing. Considering that the multipath

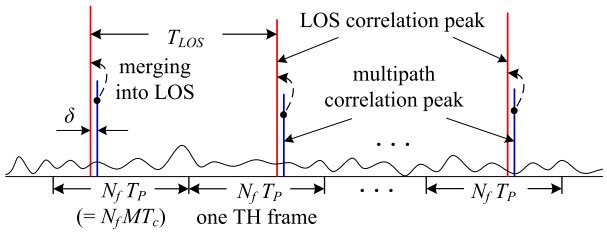

FIGURE 6. The multipath correlation peak is much close to the LOS correlation peak, which renders it can be merged into the LOS correlation peak for the detection of τ_{ip} when the conditions of the delay $\delta \ll T_p$ and the LOS peak interval between two TH frames $T_{LOS} \geq T_p$ and $T_{LOS} \leq (2N_f - 1)T_p$ are considered.

can be greatly suppressed when its delay δ exceeds one chip or T_c, if there exists a multipath after dispreading the DSSS component of the pseudolite signal, the correlation peak of the multipath will be much close to the correlation peak of the line of sight (LOS) signal, as illustrated in Fig. 6. At the same time, since that the duration of TH pulse $T_p = MT_c \gg T_c$, we can merge the multipath correlation peak into the LOS and map the merged result to value 1, thus the detection process of τ_{ip} given in Subsection III-C to III-E is still applicable.

2) COMPLEXITY OF THE GIVEN METHOD

As described in Subsection III-A, the aim of TH pulse detection is to find the PRN code initial phase τ_{fp} and the TH slot index initial phase τ_{ip}, so the computational complexity of the given method also includes two parts.

a) For τ_{fp}, based on the detection process given in Subsection III-B ($\hat{f}_{Dop}$ is set to 0 according to [19]) and the parallel PRN code phase acquisition method given in [22], its computational complexity is about $C_{prn} = \Upsilon \log(2\Upsilon)$ where $\Upsilon = \lfloor N_f f_s M / R_c \rfloor$ is the samples in one TH frame and here R_c is the PRN code rate of the pseudolite, $\log(\cdot)$ denotes base-2 logarithm.

b) For τ_{ip}, its computational complexity mainly arises from the correlation operations [19], or more specifically, the acquisition of autocorrelation peaks given in Subsection III-C and the circular correlation of two mapped code sequences $\bar{\mathbf{H}}$ and $\bar{\mathbf{\Gamma}}$ given in Subsection III-E.

During the acquisition of autocorrelation peaks of the DSSS component with the obtained τ_{fp}, if we neglect some simple operations such as data shift, data accumulation and so on, the computational complexity of this process is about $C_{autcor} = K\Upsilon$. Whereas for the circular correlation of $\bar{\mathbf{H}}$ and $\bar{\mathbf{\Gamma}}$, based on Eq. (12) its computational complexity is about $C_{circor} = NKN_f I + (3NKN_f I/2)\log(KN_f I)$ where N is the total groups of TH slot indices given in TH table and I is the interpolation factor.

Based on the above results, the total computational complexity of the given method is

$$\begin{aligned} C_{total} &\approx C_{prn} + C_{autcor} + C_{circor} \\ &= \Upsilon \log(2\Upsilon) + K\Upsilon + NKN_f I \\ &\quad + (3NKN_f I/2)\log(KN_f I) \end{aligned} \tag{13}$$

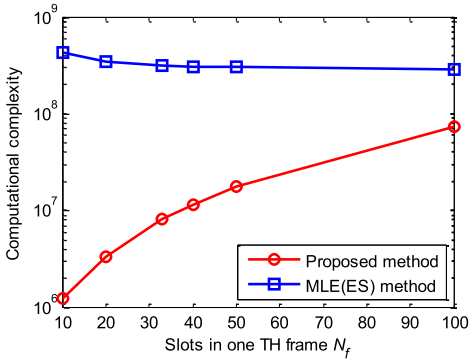

FIGURE 7. Complexity comparison of the proposed method and the exhaustive search (ES) based MLE method given in [19].

For the MLE method given in [19], with the notations given in this paper, its computational complexity of the correlation operations can be derived as

$$C'_{total} \approx K\Upsilon^2 / N_f \tag{14}$$

With the values of each parameter set up in the following Subsection IV, the simulated results of Eqs. (13) and (14) under different pulse schemes are shown as Fig. 7.

From Fig. 7, it can be seen that the computational complexity of the given method is superior to that of the exhaustive search based MLE method.

IV. NUMERICAL SIMULAIONS OF THE GIVEN METHOD

To verify the effectiveness of the given method, numerical simulations on DSSS component acquisition, detections of TH slot indices and their initial phase, probability and error of the detected initial phase of TH pulse positions under different duty cycle and different SNR are presented. The common parameters used in these simulations are set up as follows.

- Sampling frequency of the received pseudolite signal $f_s = 16.3696$ MHz, intermediate frequency $f_{IF} = 4.309$ MHz, and carrier Doppler frequency caused by clock drift and noise $f_{Dop} = 500$ Hz.
- The period of one TH frame is set to 1 ms, thus for the pulse scheme $d = 1/10$ (or 10%), the timeslot width $T_p = 0.1$ ms, and for the pulse scheme $d = 1/20$ (or 5%), $T_p = 0.05$ ms, similar operations for other pulse schemes. The total TH frames in pulse scheme d are set to $K = 1/d + 6$ if there is no special explanation. In pulse scheme $d = 1/10$, the first 12 groups of pseudorandom TH slot indices of Locata Subnet 1 [14] are selected in sequence to constitute the TH table (the value of each TH slot index decreases one so that they are in the range $[0, N_f - 1]$). Whereas for other pulse schemes, 12 groups of TH slot indices generated by the *randperm* function of the MATLAB® software compose the TH table.
- In all pulse schemes, the TH slot indices of the 7-th group in TH table are chosen to generate the pseudorandom TH pseudolite signal. The time delay or initial phase of TH pulse positions of the received pseudolite

signal is preset to $\tau_p = (3+220/1023)T_p$, i.e., the integral part $\tau_{ip} = 3$ timeslots and the fractional part $\tau_{fp} = 220/1023$ timeslots. During the circular correlation the interpolation factors of two different types of mapped code sequence are both set to 20.

- GPS C/A code is chosen as the PRN code of the TH pseudolite signal, but its code period and code (or chip) rate are respectively changed to T_p ms and $1.023/d$ Mchip/s in terms of the detailed TH pulse scheme. According to the given τ_p, the initial phase of PRN code is set to $\tau_c = \tau_{fp} = 220$ chips. Besides, since the period of data bit is often much longer than that of TH pulse and has little effect on pulse position detection of the TH pseudolite signal, for convenience, in simulations the value of data bit b_n is set to 1.

Other specific parameters used in different simulations will be given in places where they are needed.

A. DSSS COMPONENT ACQUIRED RESULTS

With the parameters given above and the method given in Subsection III-B, the correlation peaks of the discontinuous DSSS component and the corresponding PRN code initial phase can be acquired. The acquired results under different SNR and different duty cycle are shown as Figs. 8 and 9.

From Fig. 8 or 9 it can be seen that for the same duty cycle d, for example $d = 1/10$ in Fig. 8, when SNR of the received TH pseudolite signal is high, the autocorrelation peaks which bear the information of TH pulse positions will become better, and this can bring benefit for the subsequent TH pulse position detection. Meanwhile, by the comparisons of Figs. 8(b) and 9(b) or Figs. 8(d) and 9(d), it can be concluded that under the same SNR, when d become small the autocorrelation peaks will decrease, and this can be explained by that the power assigned to each TH pulse is decreased.

In addition, the comparisons of Figs. 9(b) and 9(d) also show that when SNR is high, the PRN code initial phase can be correctly detected, i.e., $\tau_{fp} = 220$ chips or $220/1023 = 0.2151$ timeslots which just match the prior given value, and when SNR is low, τ_{fp} will tend to be wrong, as given in Fig. 9(b).

B. DETECTION ON TH SLOT INDICES AND THEIR INITIAL PHASE

After acquiring the autocorrelation peaks of DSSS component and the PRN code initial phase, the TH slot indices and their initial phase τ_{ip} can also be got with the method given in Subsections III-C to III-E. The detected results are given as in Fig. 10.

Based on the detected group ID of TH slot indices given in Figs. 10(a) and 10(b) or in Figs. 10(c) and 10(d), it can be inferred that with the given method, the TH slot indices of the received pseudolite signal can be correctly detected in both pulse schemes $d = 1/10$ and $d = 1/20$, i.e., the detected TH slot indices are in group 7 of the TH table, even when SNR of the received pseudolite signal is relatively low, as given in Fig. 10(a) or 10(c). Meanwhile, from Fig. 10 it can be easily got that the detected initial phase of TH slot indices is 3 timeslots relative to their original positions, which also matches its preset value.

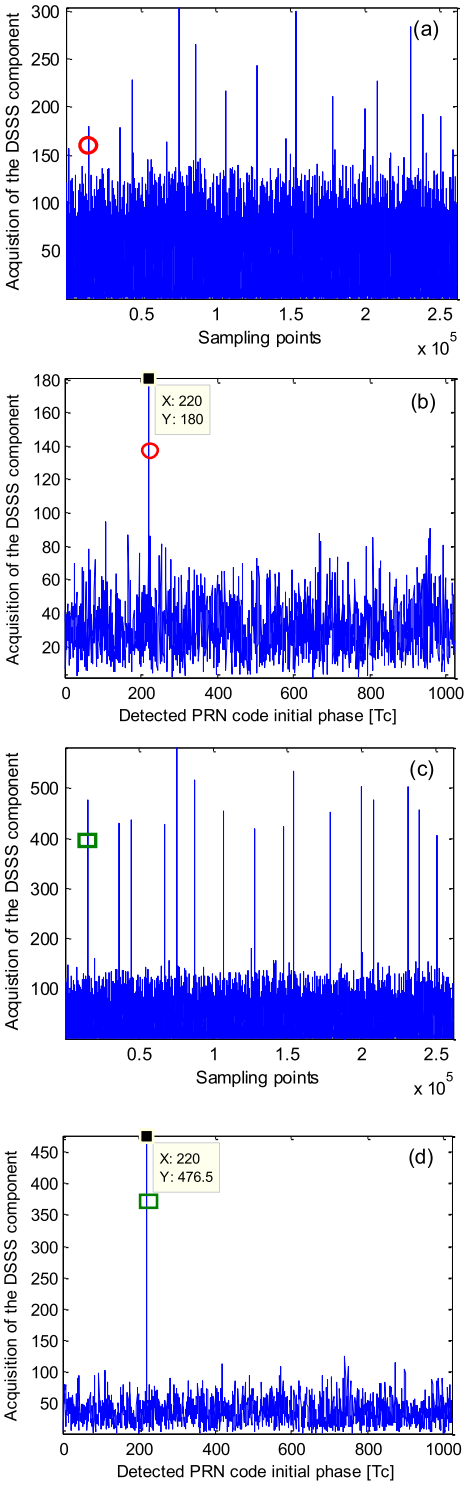

FIGURE 8. The acquisition of DSSS component and its PRN code initial phase, in which (a) and (c) are DSSS component acquired results, (b) and (d) are PRN code initial phase acquired results based on the first pulse of (a) and (c), respectively. In simulations, duty cycle $d = 1/10$ and SNR equals -12dB in (a) and (b), and -5dB in (c) and (d). The basic TH slot indices in one TH frame are [6 9 4 8 3 0 2 5 7 1] and the total TH frame number $K = 16$.

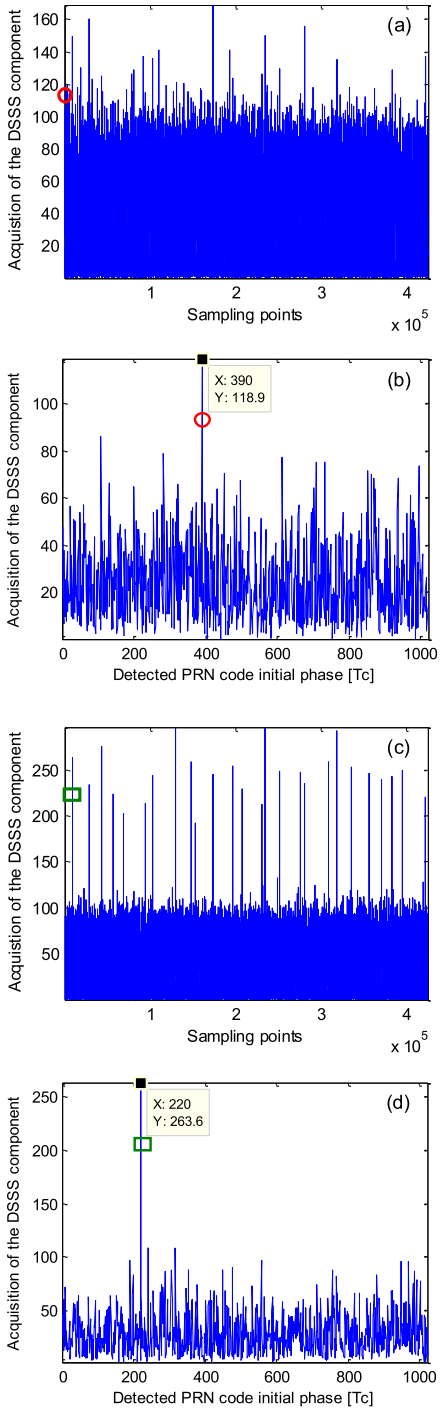

FIGURE 9. The acquisition of DSSS component and its PRN code initial phase, in which (a) and (c) are DSSS component acquired results, (b) and (d) are PRN code initial phase acquired results based on the first pulse of (a) and (c), respectively. In simulations, duty cycle $d = 1/20$ and SNR equals -12dB in (a) and (b), and -5dB in (c) and (d). The basic TH slot indices in one TH frame are [8 12 10 6 1 13 2 16 18 4 9 17 11 19 3 5 14 0 15 7] and the total TH frame number $K = 26$.

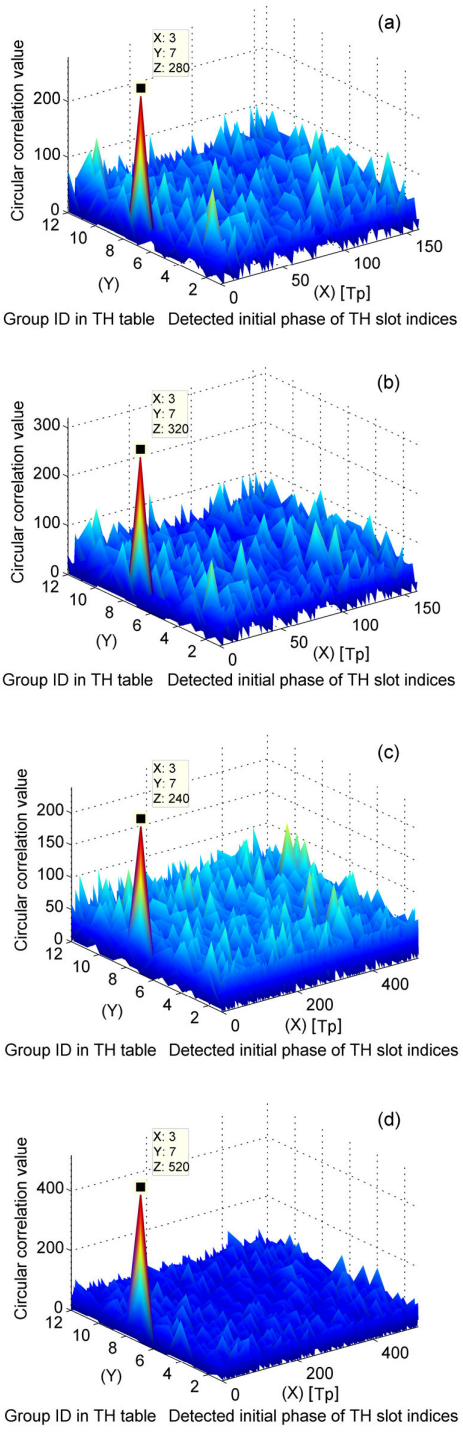

FIGURE 10. Detected TH slot indices and their initial phase under different d and different SNR, in which (a) $d = 1/10$, SNR $= -12$ dB; (b) $d = 1/10$, SNR $= -5$ dB; (c) $d = 1/20$, SNR $= -12$ dB; and (d) $d = 1/20$, SNR $= -5$ dB. Other parameters in (a) and (b) are same as those given in Fig. 8, and in (c) and (d) are same as those given in Fig. 9.

C. DETECTION ON TH SLOT INDICES AND THEIR INITIAL PHASE

With the detected PRN code initial phase τ_{fp} given in Subsection IV-A and the detected TH slot indices and their initial phase τ_{ip} given in Subsection IV-B, the final initial phase of the TH pulse positions can be obtained, hence the TH pulse positions can be easily derived aided with the TH table. The detected initial phase of TH slot indices under different duty cycle and different SNR is shown as Fig. 11.

From Fig. 11 it indicates that for smaller d, the detected initial phase of TH slot indices will become not accurate when SNR becomes relatively low, as shown in Fig. 11(c), and this will incur the incorrect determination of the TH pulse positions. The main reason of this is that the detected PRN

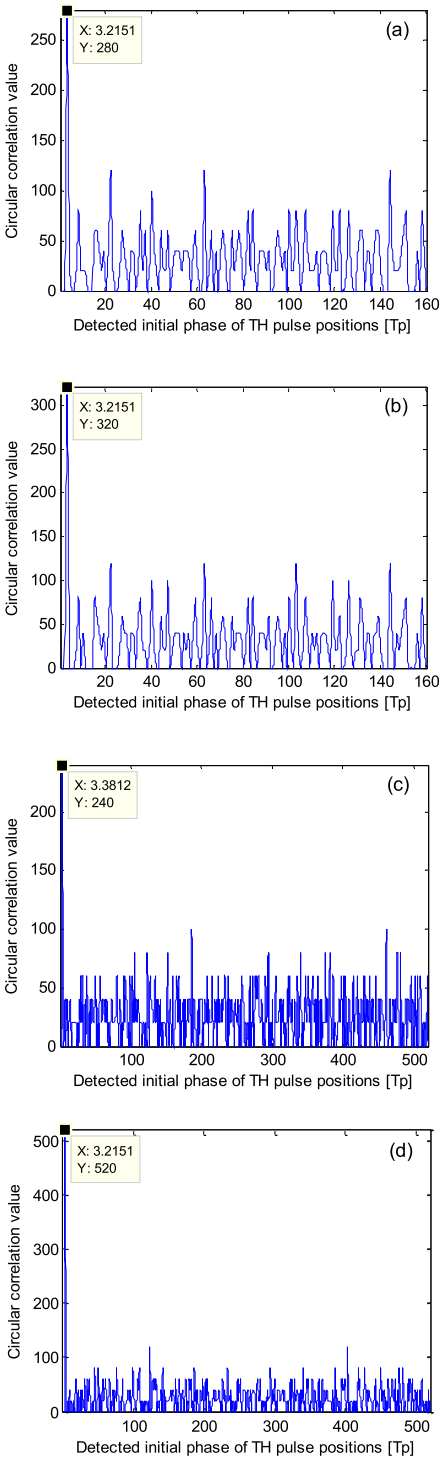

FIGURE 11. Detected initial phase of TH pulse positions under different d and different SNR, in which (a) $d = 1/10$, SNR $= -12$ dB; (b) $d = 1/10$, SNR $= -5$ dB; (c) $d = 1/20$, SNR $= -12$ dB; and (d) $d = 1/20$, SNR $= -5$ dB. Other parameters in (a) and (b) are same as those given in Fig. 8, and in (c) and (d) are same as those given in Fig. 9.

code initial phase τ_{fp} is more sensitive to SNR of the received pseudolite signal, as shown in Figs. 9(a) and 9(b).

D. PERFORMANCE ON DETECTION PROBABILITY AND DETECTION ERROR

To further verify the performance of the given method, detection probability and standard deviation (SD) of the detected

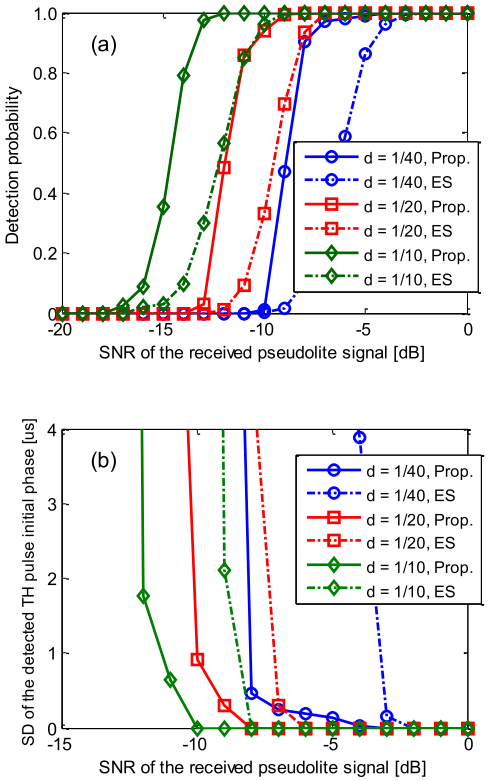

FIGURE 12. Performance comparisons of the detected initial phase of TH pulse positions with the proposed method (Prop.) and with the ES method, in which (a) is the detection probability and (b) is the standard deviation (SD) of the detected TH pulse initial phase. Here $K = 1/d + 6$.

TH pulse initial phase are simulated with Monte Carlo method, and the results are shown in Figs. 12 and 13, in which the frame number K equals $1/d + 6$ in Fig. 12 and $1/d + 18$ in Fig. 13. The simulation runs in Figs. 12 and 13 are both 1000. Besides, the simulated results of the exhaustive search (ES) method [18] under the same conditions are also given for comparisons. Here the reason that SD of the detected TH pulse initial phase is chosen to be estimated is because the TH pulse positions are determined by their initial phase τ_p aided with the TH table stored in the participative GNSS receivers, as illustrated in Subsection III-A.

From Fig. 12(a) or 13(a) it can be seen that when the duty cycle d decreases, the probability of acquiring the right TH initial phase with the given method and the ES method will both become poor, but the proposed method is still superior to the ES method at this time. For example, in Fig. 12(a), under the conditions of $d = 1/20$ and detection probability equals 0.8 (or 80%), the SNR of the given method is lower than that of the ES method about 3 dB. Similar result can also be found in Fig. 13(a). In addition, by comparing Fig. 12(a) and 13(a) it also shows that under the same SNR and d, when the frame number K increases, the detection probability of the two methods will also increase. However, at this time the computational complexity of the two methods will also increase, so we should make a tradeoff between detection performance and computational complexity.

While in Fig. 12(b) and 13(b), there are similar results as those in Fig. 12(a) and 13(a). For example, in Fig. 12(a),

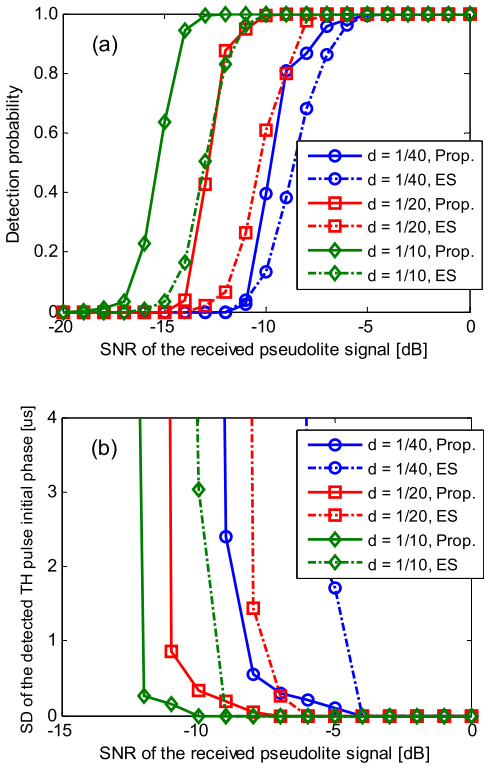

FIGURE 13. Performance comparisons of the detected initial phase of TH pulse positions with the proposed method (Prop.) and with the ES method, in which (a) is the detection probability and (b) is SD of the detected TH pulse initial phase. Here $K = 1/d + 18$.

under the condition $d = 1/20$, with the given method SD of the detected initial phase of TH pulse positions will decease to 0 when SNR equals -8 dB; whereas with the ES method it will decrease to 0 when SNR equals -6 dB. That is, the former is superior to the latter about 2 dB in SD performance. The similar results can also be found in Fig. 13(b) and in other pulse schemes. In addition, the simulated results given in Figs. 12(b) and 13(b) also indicate that when K increases, the SD performance of the detected TH pulse positions of the two methods will also get improved, just as it in Figs. 12(a) and 13(a).

V. CONCLUSION

A new method to detect the pseudorandom TH pulse positions of the received pseudolite signal for the participative GNSS receivers is given. In the given method, the TH intervals derived from the correlation peaks of discontinuous DSSS component are first mapped to a code sequence, and then the mapped code sequence is circularly correlated with the code sequences obtained from the TH slot indices of the stored TH table, finally by searching the maximum circular correlation peak, the TH slot indices of the received pseudolite signal and their initial phase will be found, further by combining them the work of TH pulse detection is fulfilled. With the given method, the effect of some unmatched TH intervals can be greatly decreased, and consequently the detection probability and detection error of the obtained TH pulse positions are improved, which will bring benefit to the ranging and demodulation performance of the participative GNSS receivers. Additionally, by combining with the code division multiple access function of the PRN code, the given method can also be generalized to detect the TH pulse positions of multiple pseudolite signals.

REFERENCES

[1] J. Wang, "Pseudolite applications in positioning and navigation: Progress and problems," *J. Global Positioning Syst.*, vol. 1, no. 1, pp. 48–56, Jun. 2002.
[2] H. Oktay and M. Stepaniak, "Airborne pseudolites in a global positioning system degraded environment," in *Proc. 5th Int. Conf. Recent Adv. Space Technol.*, Istanbal, Turkey, Jun. 2011, pp. 280–285.
[3] C. Kim, H. So, T. Lee, and C. Kee, "A pseudolite-based positioning system for legacy GNSS receivers," *Sensors*, vol. 14, no. 4, pp. 6104–6123, Mar. 2014.
[4] S. Ganguly, A. Jovancevic, M. Kirchner, J. Noronha, and S. Zigic, "GPS signal reconstitu- tion," in *Proc. 17th Int. Tech. Meeting Satell. Division*, Long Beach, CA, USA, Sep. 2004, pp. 592–603.
[5] M. G. Farley and S. G. Carlson, "A new pseudolite battlefield navigation system," in *Proc. IEEE Position Location Navigat. Symp.*, Palm Springs, CA, USA, Aug. 1998, pp. 208–217.
[6] S. H. Cobb, "GPS pseudolites: Theory, design and applications," Ph.D. dissertation, Stanford Univ., Stanford, CA, USA, 1997. [Online]. Available: http://web.stanford.edu/group/scpnt/gpslab/pubs/theses/StewartCobbThesis97.pdf
[7] P. H. Madhani, P. Axelrad, K. Krumvieda, and J. Thomas, "Application of successive interference cancellation to the GPS pseudolite near-far problem," *IEEE Trans. Aerosp. Electron. Syst.*, vol. 39, no. 2, pp. 481–488, Apr. 2003.
[8] K. Barltrop, J. Stafford, and B. Elrod, "Local DGPS with pseudolite augmentation and implementation considerations for LAAS," in *Proc. 9th Int. Tech. Meeting Satell. Division*, Sep. 1996, pp. 449–459.
[9] F. S. Eads Astrium, "Theoretical approach for the optimization of pseudolite pulsing scheme and the implementation of participative receivers," in *Proc. 6th ESA Workshop Satell. Navigat. Technol.*, Noordwijk, The Netherlands, Dec. 2012, pp. 1–8.
[10] D. Borio and C. Odriscoll, "Design of a general pseudolite pulsing scheme," *IEEE Trans. Aerosp. Electron. Syst.*, vol. 50, no. 1, pp. 2–16, Jan. 2014.
[11] T. L. Abt, F. Soualle, and S. Martin, "Optimal pulsing schemes for Galileo pseudolite signals," *Positioning*, vol. 1, no. 12, pp. 133–141, Dec. 2007.
[12] B.-L. Zhou, B.-G. Yu, and W.-X. Luo, "A new approach for pulsed pseudolite signal acquisition using FFT," in *Proc. 9th Int. Conf. Signal Process.*, Beijing, China, Oct. 2008, pp. 2909–2912.
[13] T. A. Stansell, "RTCM SC-104 recommended pseudolite signal specification," *Navigation*, vol. 33, no. 1, pp. 42–59, Mar. 1986.
[14] *Locata Signal Interface Control Document, Locata-ICD-100E*, Locata Corp., Griffith, Australia, 2014.
[15] S. Yun, Z. Yao, T. Wang, and M. Lu, "High accuracy and fast acquisition algorithm for pseudolites-based indoor positioning systems," in *Proc. 4th Int. Conf. Ubiquitous Positioning, Indoor Navigat. Location Based Services*, Shanghai, China, Nov. 2016, pp. 51–60.
[16] J. Wang, Y. Xu, R. Luo, Y. Zhang, and H. Yuan, "Synchronisation method for pulsed pseudolite positioning signal under the pulse scheme without slot-permutation," *IET Radar, Sonar Navigat.*, vol. 11, no. 12, pp. 1822–1830, Dec. 2017.
[17] A. J. Van Dierendonck, P. Fenton, and C. Hegarty, "Proposed airport pseudolite signal specification for GPS precision approach local area augmentation systems," in *Proc. 10th Int. Tech. Meeting Satell. Division*, Kansas City, MO, USA, Sep. 1997, pp. 1603–1612.
[18] J. Cheong, A. G. Dempster, and C. Rizos, "Detection of time-hopped DS-CDMA signal for pseudolite-based positioning system," in *Proc. 22nd Int. Tech. Meeting Satell. Division*, Savannah, GA, USA, Sep. 2009, pp. 881–891.
[19] D. Borio, E. Cano, and G. Baldini, "Synchronization of pulsed pseudolite signals: Analysis and comparison," in *Proc. Int. Tech. Meeting Satell Division*, Nashville, TN, USA, Sep. 2012, pp. 482–493.
[20] T. Wu, X. Zhan, and X. Zhang, "Transceiver pseudolite carrier frequency self-alignment closed-loop system," *Aerosp. Syst.*, vol. 3, no. 1, pp. 41–52, Mar. 2020.
[21] G. He, M. Song, X. He, and Y. Hu, "GPS signal acquisition based on compressive sensing and modified greedy acquisition algorithm," *IEEE Access*, vol. 7, pp. 40445–40453, 2019.

[22] K. Borre, D. M. Akos, N. Bertelsen, P. Rinder, and S. H. Jensen, *A Software-Defined GPS and Galileo Receiver: A Single-Frequency Approach*. Boston, MA, USA: Birkhäuser, 2006.
[23] X. Chen, F. Dovis, and M. Pini, "An innovative multipath mitigation method using coupled amplitude delay lock loops in GNSS receivers," in *Proc. IEEE/ION Position, Location Navigat. Symp.*, Indian Wells, CA, USA, May 2010, pp. 1118–1126.
[24] B. R. Townsend, P. C. Fenton, K. J. Van Dierendonck, and R. D. J. Van Nee, "Performance evaluation of the multipath estimating delay lock loop," *J. Inst. Navig.*, vol. 42, no. 3, pp. 503–514, Oct. 1995.
[25] M. Sahmoudi and M. Amin, "Fast iterative maximum-likelihood algorithm (FIMLA) for multipath mitigation in the next generation of GNSS receivers," *IEEE Trans. Wireless Commun.*, vol. 7, no. 11, pp. 4362–4374, Nov. 2008.

YI HU was born in Lu'an, China, in 1974. He received the Ph.D. degree in communications and information system from the Nanjing University of Aeronautics and Astronautics (NUAA), in 2015.

He is currently an Associate Professor with the School of Mechanical and Electrical Engineering, Chuzhou University. His research interests include satellite navigation signal processing techniques, cognitive positioning, and satellite communications.

BAOGUO YU was born in Inner Mongolia, China, in 1966. He received the Ph.D. degree in satellite navigation engineering from the Beijing Institute of Technology (BIT), in 1995.

He is currently a Director and Research Professorship with the State Key Laboratory of Satellite Navigation System and Equipment Technology. His research interests include satellite navigation signal processing techniques, software defined GNSS receiver design and applications, and satellite communications.

MAOZHONG SONG was born in Shexian, China, in 1962. He received the M.S. degree in communications and electronic system from Zhejiang University, China, in 1986.

He has been with the College of Electronic and Information Engineering, NUAA, since 1986, where he is currently a Professor. His research interests include wireless communications and satellite navigation, with a focus on modulation signal design and signal processing techniques.

ZHIXIN DENG was born in Harbin, China, in 1982. He received the M.S. and Ph.D. degrees in navigation, guidance and control from Harbin Engineering University, in 2008, and 2009, respectively.

Since 2009, he has been working with the State Key Laboratory of Satellite Navigation System and Equipment Technology, and he is currently a Senior Engineer. His research interests include satellite navigation signal processing techniques and wireless communications.